Handover-Related Self-Optimization in Femtocells: A Survey and an Interaction Study

Article *in* Computer Communications · August 2015

DOI: 10.1016/j.comcom.2015.08.013

CITATIONS
9

READS
373

3 authors, including:

Kais Elmurtadi Suleiman
University of Waterloo
9 PUBLICATIONS **27** CITATIONS
SEE PROFILE

Hossam S. Hassanein
Queen's University
613 PUBLICATIONS **8,434** CITATIONS
SEE PROFILE

Handover-Related Self-Optimization in Femtocells: A Survey and an Interaction Study

Kais Elmurtadi Suleiman[a], Abd-Elhamid M. Taha[b,*], Hossam S. Hassanein[c]

[a] *Electrical and Computer Engineering, University of Waterloo, Waterloo, Canada*
[b] *Electrical Engineering, Alfaisal University, Riyadh, KSA*
[c] *School of Computing, Queen's University, Kingston, Canada*

Abstract

Femtocells enable LTE technology when deployed in large numbers. However, every femtocell needs to self-optimize its control parameters in response to surrounding dynmaic events. This paper focuses on self-optimization use cases related to handovers in LTE femtocell networks including: handover self-optimization, call admission control self-optimization and load balancing self-optimization. These three use cases can interact either constructively or destructively. To the best of our knowledge, no previous work has addressed the nature of this interaction. Therefore, we survey proposed schemes for each one of these handover-related self-optimization use cases after which three representative schemes have been identified. These schemes are used in our interaction study using our in-house MATLAB-written and LTE compliant simulation environment. Based on interaction simulation results, we recommend a set of guidelines to follow when coordinating between these interacting handover-related self-optimization use cases in LTE femtocell networks.

Keywords: LTE, Self-optimization, Handover, Simulation, Femtocell.

1. Introduction

The notion behind femtocells is to bring the network closer to users. With this approach, femtocells overcome the disadvantage of macrocells which usually struggle to provide services for the 50% of voice calls and the 70% of data calls originating indoors [1]. There are estimates that with as low as 10% of active femtocell household deployment, femtocells can offload as much as 50% of the overall macrocellular tier load [2] and therefore increase mobile operator revenues. Motivated by such benefits, femtocells are expected to reach as high as 28 million units by 2017 [3]. If these estimations were correct, several technical

*Corresponding author
Email addresses: kelmurta@uwaterloo.ca (Kais Elmurtadi Suleiman), ataha@alfaisal.edu (Abd-Elhamid M. Taha), hossam@cs.queensu.ca (Hossam S. Hassanein)

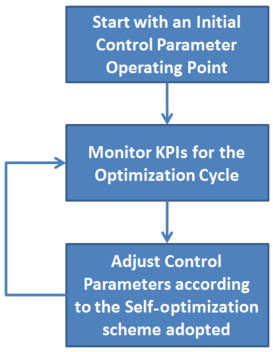

Figure 1: Self-optimization Scheme Cycle.

issues would need to be addressed. One major challenge is the instant control parameter adjustments needed in response to surrounding dynamic events. These adjustments can be made automatically by implementing Self Organizing Network (SON) use cases categorized into: self-configuration, self-optimization and self-healing. The term "use case" indicates implementation of SON capabilities to address a certain area (e.g. handover). Several schemes can fall within a single SON use case.

In this work, we focus on self-optimization use cases related to the LTE femtocell handover procedure. These use cases start by virtually adjusting the femtocell's coverage footprint by implementing handover self-optimization and load balancing self-optimization. These use cases control gaps and femtocell coverage overlaps which in turn controls handover decisions initiation at source cells. Target cells can also grant or reject these handover decisions by implementing call admission control self-optimization. Each one of these three handover-related self-optimization use cases starts with an initial operating point defined by control parameters. After that, each use case monitors Key Performance Indicators (KPI) and reacts by adjusting its control parameters in order to meet performance objectives in terms of the same KPIs monitored. This self-optimization cycle is shown in Figure 1.

As it can be noticed, all of the self-optimization use cases mentioned above improve the same handover process. Therefore, their adjustment decisions can either interact positively or negatively. To the best of our knowledge, no work has ever addressed the issue of interaction between these handover-related self-optimization use cases in LTE femtocell networks, namely: handover self-optimization, call admission control self-optimization and load balancing self-optimization. As an extension to our previous work in [4] and [5], this paper addresses in more details for the first time this interaction issue after conducting a thorough survey of proposed handover-related self-optimization schemes. This is achieved using our in-house MATLAB-written and LTE compliant simulation environment.

This paper starts by giving some background knowledge in Section 2 in-

cluding how the standard LTE handover procedure works and how various self-optimization network architectures can be implemented in such a procedure. In addition, we explain in this section in more details the three handover-related self-optimization use cases of interest after defining some of the most commonly used KPIs. These explanations show the main issue of possible interactions addressed in this study.

In Section 3, we show first the need for our interaction study. Then we survey proposed handover, call admission control and load balancing self-optimization schemes in order to identify a representative scheme for each use case. Interactions are studied with these representative schemes using simulations. However, and before introducing the simulation experiments, we introduce in Section 4 our simulation environment after which experiments are given in Section 5. Results are discussed further in Section 6 in addition to giving some interacting scheme coordination guidelines. Finally, Section 7 concludes the paper.

2. Background

2.1. LTE Handover Procedure

LTE handover procedure has three phases: preparation, execution and completion. The last two phases provide commands for data loss detection and recovery which are out of our research scope in this paper. However, our focus is on the handover preparation phase as shown in Figure 2. In what follows, we elaborate on steps 4, 6 and 8 at which handover-related use cases operate by self-optimizing control parameters for instance.

2.1.1. UE Measurements and Decision

According to [6], source eNB/HeNB initially configures the way by which UEs report their proximity. When the UE sends a proximity indication, source eNB/HeNB can configure the UE with the most recent measurement configurations. These configurations may include a list of all neighbouring cells which helps the UE in performing a faster and less battery consuming scanning. If this list was not provided, then the UE would just detect those cells with a Reference Signal Received Power (RSRP) exceeding the UE's receiver sensitivity. These measurement configurations also include the rules by which the UE should start taking or stop taking any further measurements. In general, taking these measurements could be event triggered or periodically triggered. According to [7], there are eight types of events that could trigger the UE to start reporting the measurements:

1. **Event A1:** is when the serving cell becomes better, in terms of signal strength or quality, than a threshold.
2. **Event A2:** is when the serving cell becomes worse, in terms of signal strength or quality, than a threshold.
3. **Event A3:** is when a neighbouring cell becomes offset better, in terms of signal strength or quality, than the Primary Cell. Primary cells are relevant if the network system aggregates carriers.

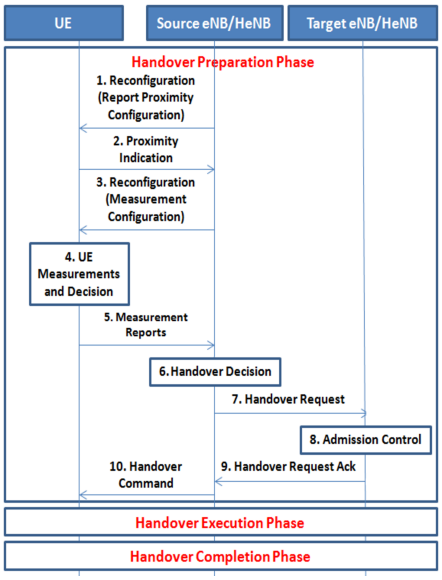

Figure 2: Overall LTE Handover Procedure.

4. **Event A4:** is when a neighbouring cell becomes better, in terms of signal strength or quality, than a threshold.
5. **Event A5:** is when the Primary Cell becomes worse than threshold-1 while having a neighbour cell that has become better than threshold-2, and that is in terms of signal strength or quality.
6. **Event A6:** is when a neighbouring cell becomes offset better, in terms of signal strength or quality, than the Secondary Cell. Secondary cells are relevant if the network system aggregates carriers.
7. **Event B1:** is when an inter Radio Access Technology (RAT) neighbouring cell becomes better, in terms of signal strength or quality, than a threshold.
8. **Event B2:** is when the Primary Cell becomes worse than threshold-1 while having an inter-RAT neighbouring cell that has become better than threshold-2, and that is in terms of signal strength or quality.

In **RRC IDLE state**, the UE makes its own cell selection decisions and it will initially seek to "camps on" a suitable cell that has the highest RSRP. After that, the UE reselects another suitable cell if it has a higher RSRP. If no suitable cell is found, then the UE will seek to identify an acceptable cell that allows the UE to initiate emergency calls and receive warning messages.

Transitioning from RRC IDLE state to RRC CONNECTED state starts by the time the user initiates a call. The UE starts by selecting the neighbouring target cell with the highest RSRP. If this UE selection request was rejected, then a barring timer would be triggered and the UE would return back to RRC IDLE state. If the user has managed to get access to another target cell, the timer will reset .

In **RRC CONNECTED state**, the UE measurements include: RSRP levels, physical cell identities, cell global identities, closed subscriber group IDs and member Indications. Knowing target cell unique global identities prevents report confusions between the many femtocells expected to be deployed. Moreover, knowing cell subscriber group IDs and member Indications is also needed when dealing with different femtocell access schemes. Finally, RSRP measurements are needed by source eNB/HeNB when making handover decisions.

Next handover procedure step shows how these UE measurements assist source eNB/HeNB in making its final handover decision and target eNB/HeNB in making its final admission control decision.

2.1.2. Handover Decision

According to [8], a handover request is sent to the target cell that has the highest signal strength level, if the user has spent at least 1 second at the current serving cell and the following condition is met for a duration of *TReselection*:

$$Q_{meas,n} > Q_{meas,s} + Q_{offset_{s,n}} + Q_{Hyst_s}$$

Where:

$Q_{meas,n}$	is the neighbouring cell RSRP in dBm.
$Q_{meas,s}$	is the serving cell RSRP in dBm.
$Q_{offset_{s,n}}$	is the neighbouring cell individual offset as stored in the serving cell in dB.
Q_{Hyst_s}	is the serving cell handover hysteresis margin in dB.

According to [9], Q_{Hyst} and TReselection can be scaled based on user mobility state. This state is decided by comparing the number of UE cell reselections occurring within a predefined duration against predefined thresholds. Three mobility state outcomes can occur: high, medium and normal. In addition, both Q_{Hyst} and TReselection can affect handovers globally. However, Q_{offset} can affect only those handovers between a source cell and a specific neighbouring cell.

2.1.3. Admission Control

There are three main access schemes in LTE femtocell networks:

- **Closed:** where subscribers benefit from having secure and exclusive access rights.
- **Open:** where every user is allowed access which compromises service quality and security.
- **Hybrid:** which tries to harness the benefits of both closed and open access schemes.

Depending on the access scheme adopted by the target cell, the UE's handover request can either be denied or granted access. If the request is denied, then

we will have a **Handover Failure**. Successive handover failures could lead to a **Radio Link Failure**. If the handover request is granted, then handover execution phase followed by handover completion phase will be triggered. If the user spends less than 5 seconds in the target cell(s) before returning back to the same source cell, then we will have a **Ping Pong Handover**.

2.2. Self-optimization Network Architecture

According to the SON concepts and requirements specified by 3GPP in [10], self-optimization use cases can logically be implemented as a centralized, distributed or hybrid architecture. In centralized architectures, algorithms run within the core network operations, administration and management element. On the other hand, algorithms run locally at each eNB/HeNB in distributed architectures. In hybrid architectures, algorithms run both centrally at the core network and locally at each eNB/HeNB. None of these architectures have UEs hosting any significant self-optimization functionalities (i.e. all functionalities are placed at the network side). This placement is done purposefully to allow for an economic and maintainable implementation.

2.3. Handover-related Self-optimization

Before elaborating on the three handover-related self-optimization use cases of interest, we define some commonly used KPIs as follows:

- **Handover Failure Ratio (HOFR):** which is the ratio between the number of handover failures and the total number of handovers including handover failures and successful handovers.
- **Ping Pong Handover Ratio (PPHOR):** which is the ratio between the number of ping pong handovers and the total number of handovers. Notice that successful handovers include ping pong handovers.
- **Call Dropping Probability (CDP):** which is the ratio between the number of radio link failures and the number of accepted calls. Notice that accepted calls include newly initiated calls from within the cell and calls previously handed over to the cell.
- **Call Blocking Probability (CBP):** which is the ratio between the number of call blocks and the summation of newly accepted calls and call blocks.

Now, we can explain the use cases of interest as follows:

- **HandOver Self-Optimization (HO-SO):** this use case takes place at the source cell to decrease HOFR, PPHOR and CDP. Otherwise, tradeoffs are made.
- **Call Admission Control Self-Optimization (CAC-SO):** this use case takes place at the target cell to admit as many calls as possible while maintaining an acceptable level of service for ongoing calls. This usually decreases HOFR and CDP at the cost of increasing CBP.

- **Load Balancing Self-Optimization (LB-SO):** this use case takes place at the source cell to balance network load by forcing it to move from overutilized cells to underutilized cells. This decreases HOFR and CBP but increases PPHOR. It can also increase CDP since load is usually forced to move from overutilized cells with higher power levels to underutilized cells with lower power levels.

2.4. Self-optimization Use Case Interactions

In order to implement these handover-related self-optimization use cases, several schemes can be adopted where various KPIs and control parameters can be used. As explained, each use case has its own strategy on how the handover process should be enhanced. They affect almost the same KPIs which would lead them to interact. Negative interactions occur when a scheme contradicts or limits the benefits of others, whereas positive interactions occur when schemes help each other improve the overall network performance.

3. Related Work

We start with a survey of related interaction studies to show the need for our work. After that, we continue by surveying proposed and relevant handover-related self-optimization schemes in order to identify a representative scheme for each use case. The resulting three representative schemes are carried forward in the next sections as part of our interaction study.

3.1. Interaction Studies

Interaction between HO-SO and LB-SO is studied in [11]. The HO-SO scheme adjusts Q_{Hyst} and TReselection when triggered by high HOFR, CDP or PPHOR. Whereas, the LB-SO scheme adjusts $Q_{offsets}$ when triggered by neighbouring cells load differences. Both schemes run periodically with a shorter LB-SO interval compared to HO-SO. This leads LB-SO to dominate over HO-SO especially in overload conditions. Therefore, both [12] and [13] propose that HO-SO should be stopped from triggering backward handovers after having LB-SO shifting load from overloaded cells.

Authors in [14] study HO-SO and CAC-SO interaction. The HO-SO scheme monitors periodically the trend followed by a weighted summation of HOFR, CDP and PPHOR. If this summation is decreasing, then the same optimization direction is followed and the next operating point defined by Q_{Hyst} and TReselection is selected and vice versa. For the CAC-SO scheme, the conventional guard channel policy is adopted with a dynamic threshold. This threshold is decreased if HOFR or the ratio of calls with a low throughput is higher than a predetermined value. If both of these KPIs are lower than this value and CBP is higher than another predetermined value, then the guard channel policy threshold is increased. In any other case, this threshold does not change. Both schemes are interacting constructively in terms of achieving lower HOFR and lower CDP, while no effect is taking place in terms of PPHOR. Moreover, the

CAC-SO scheme benefits by blocking less calls. The authors in [14] conclude that the overall interaction is positive.

Finally, and to the best of our knowledge, no further interaction studies have been published for any combination of the three handover-related self-optimization use cases of interest. This has led us to conduct the following surveys.

3.2. Handover Self-optimization

3.2.1. Survey of Schemes

Authors in [15] propose a scheme that monitors current cell load and type. Without adjusting a specific control parameter, authors propose an empirical formula to modify received UE RSRP measurements. These modified measurements make handover decisions react to current cell load and type while being triggered by RSRP differences as given in [16]. Therefore, handover decisions are initiated towards cells with higher RSRP. Using these modified RSRP measurements affects handover decisions and therefore cell loads.

Other schemes adjust standardized control parameters including Q_{Hyst}, TReselection and $Q_{offsets}$. In [17], an HO-SO scheme adjusts either Q_{Hyst} or TReselection in reaction to handover defect types including too early handovers, too late handovers and handovers to wrong cells. The scheme differentiates between these defects by measuring their resulting HOFR, PPHOR and CDP. Based on these measurements, a decision is made on how to adjust either Q_{Hyst} or TReselection where the adjustment step size is a function of the average failure ratio.

Contrary to [17], authors in [18] choose Q_{offset} instead of TReselection since Q_{offset} is cell-pair specific which gives more flexibility in triggering handovers. They find that depending on user mobility, different handover defect types dominate. Therefore, their scheme decides first which handover defect type dominates by monitoring first too early handovers, too late handovers, handovers to wrong cells and ping pong handovers. After that, it reacts to user mobility causing this handover defect dominance by adjusting the corresponding $Q_{offsets}$.

A multi-control parameter adjusting scheme is proposed by [19]. The scheme starts by exchanging with neighbouring cells the number of radio link failures, the number of too early handovers and the number of handovers to wrong cells. If the total summation of these events exceeds a predefined threshold, then the scheme checks whether a global or a local optimization is necessary. If global optimization is necessary, then Q_{Hyst} and TReselection are adjusted. However, if local optimization is enough, then only relevant $Q_{offsets}$ are adjusted. These adjustments are made based on monitored KPIs and weights given to them by the operator policy.

Three multi-control parameter adjusting schemes are proposed in the European Union project of Self Optimization and self ConfiguRATion in wirelEss networkS (SOCRATES) [11]. These schemes are: the Simplified Trend-based scheme, the Trend-based scheme and the Handover Performance Indicator Sum-based scheme.

The Simplified Trend-based scheme monitors periodically HOFR, CDP and PPHOR. The trend followed by each KPI is determined by comparing its current value against its predefined threshold. Based on the trend detected, both Q_{Hyst} and TReselection are adjusted. For instance, if both HOFR and PPHOR are lower than their thresholds and CDP is higher than its threshold, then both Q_{Hyst} and TReselection will be decreased and vice versa. However, if all KPIs are higher than their thresholds, then all thresholds are increased and vice versa.

Contrary to the Simplified Trend-based scheme, the Trend-based scheme does not run periodically. It compares current KPI measurements against their thresholds and waits for the comparison result to hold for a predefined duration. If these KPI measurements are lower than their thresholds, then a "good performance" is detected and the corresponding KPI thresholds are decreased. On the other hand, if these KPI measurements are higher than their thresholds, then a "bad performance" is detected and the scheme either changes Q_{Hyst} and TReselection or increases KPI thresholds. As discussed in [20], the empirical criteria for changing Q_{Hyst} and TReselection is developed after conducting a sensitivity analysis for each KPI against all Q_{Hyst} and TReselection combinations.

The Handover Performance Indicator Sum-based scheme monitors periodically an indicator that is defined as a weighted summation of HOFR, CDP and PPHOR. It compares current indicator value against its last value. If the value is decreasing, then the same optimization direction is followed and vice versa. The same empirical criteria mentioned in [20] is adopted for this scheme. The drawback here is that any slight handover performance indicator change may cause a change in the optimization direction needlessly. Therefore, reference [21] proposes preventing the optimization direction from switching unless the indicator change percentage is higher than a threshold called the "Performance Degradation Percentage" (PDP). A T-test is proposed in [22] to be implemented just before this PDP strategy to determine the statistical significance of the difference between current and last handover performance indicator values. These improvements yields the Enhanced Handover Performance Indicator Sum-based scheme [22].

3.2.2. Representative Scheme

Surveyed HO-SO schemes are summarized as shown in Table 1 where the Simplified Trend-based scheme proposed by [11] is chosen as our HO-SO representative scheme for the following reasons:

- It is a multi-control parameter adjusting scheme, which gives more flexibility in altering handover decisions,
- Both Q_{Hyst} and TReselection are commonly used standardized control parameters,
- It is generic and does not rely on any empirical formula,
- Lastly, it is based on monitoring locally processed KPI measurements with no signalling needed.

Table 1: Handover Self-optimization Schemes Summary.

Scheme	Control Parameters	Technique	SON Architecture
H. Zhang et al. [15] scheme.	Not Applicable	Adjusting UE RSRP measurements in response to cell load and type.	Distributed
C. Feng et al. [17] scheme.	Q_{Hyst} or TReselection	Comparing KPIs to decide the handover defect type.	
K. Kitagawa et al. [18] scheme.	$Q_{offsets}$	Monitoring handover events to detect dominant defect type.	Centralized or Hybrid
L. Ewe et al. [19] scheme.	Q_{Hyst} and TReselection or $Q_{offsets}$	Collecting number of events to decide whether a global or local optimization is needed.	
T. Kürner et al. [11] Simplified Trend-based scheme.	Q_{Hyst} and TReselection	Comparing KPIs against their thresholds to detect trends.	Distributed
T. Kürner et al. [11] Trend-based scheme.		Comparing KPIs against their thresholds and wait for trend to hold. Adjustments are made according to an empirical criteria.	
T. Kürner et al. [11] Handover Performance Indicator Sum-based scheme.		A weighted KPI summation trend is detected on which adjustments are made according to an empirical criteria.	
I. Balan et al. [22] Enhanced Handover Performance Indicator Sum-based scheme.		The Handover Performance Indicator Sum-based scheme is enhanced by not responding to minor performance changes.	

Algorithm 1 HO-SO Representative Scheme [11].

```
1.  Initialize HOFR_TH, CDP_TH and PPHOR_TH
2.  while Cell is ON do
3.    if an optimization interval has passed then
4.      Compute optimization interval HOFR, CDP and PPHOR
5.      if HOFR<HOFR_TH and PPHOR<PPHOR_TH then
6.            if CDP>CDP_TH then
7.                Decrease Q_Hyst and TReselection;
8.            else
9.                Decrease HOFR_TH, CDP_TH and PPHOR_TH;
10.           end if
11.     else
12.           if CDP≤CDP_TH then
13.               Increase Q_Hyst and TReselection;
14.           else
15.               Increase HOFR_TH, CDP_TH and PPHOR_TH;
16.           end if
17.     end if
18.   end if
19. end while
```

Algorithm 1 shows the pseudocode for this HO-SO representative scheme. The scheme starts by initializing operator KPI thresholds. Then, it periodically measures local HOFR, CDP and PPHOR to evaluate how Q_{Hyst} and TReselection should be changed. Most importantly, this scheme trades off HOFR and PPHOR with CDP.

3.3. Call Admission Control Self-optimization

3.3.1. Survey of Schemes

All CAC-SO schemes surveyed are based on making bandwidth reservations by using non standardized control parameters. To begin with [23], authors propose a scheme that reserves resources for non-real-time calls. Authors claim that reserving resources for real-time calls would still not prevent these delay intolerant services from getting dropped, whereas reserving resources for non-real-time calls results in avoiding congestions due to their delay tolerance. The reserved bandwidth threshold is decreased, if the real-time calls packet drop rate is higher than a predetermined value, or increased otherwise.

Contrary to [23], authors in [24] and [25] propose schemes which do not differentiate between non-real-time and real-time calls but rather prioritize handover calls over new calls by adopting the conventional guard channel policy with a dynamic threshold. Both [24] and [25] adjust the same threshold in response to periodical measurements albeit differently. In [24], more resources are reserved for handovers by decreasing the threshold in response to a high HOFR. However, the threshold is increased in response to a low HOFR that lasts for a number

of successful handover attempts. This makes the scheme responds slower to low HOFRs and therefore prevents system oscillations. In general, increasing this threshold leads to a lower CBP.

Similar to [24], the scheme in [25] monitors HOFR, CBP and the fraction of calls with a low throughput. If this fraction of calls and HOFR are high, then the dynamic guard channel threshold is decreased and vice versa if these KPIs are low but CBP is high. Generally, increasing the threshold is done slower than decreasing it in order to prioritize handovers over new calls.

In another work, authors of [26] claim that users have predictable mobility habits. Therefore, a mobility prediction algorithm is proposed to derive users' handover probabilities towards neighbouring cells. Neighbouring cells, at which these probabilities pass a predefined value, are part of a cell cluster used in making admission decisions. For instance, a new call is admitted, if the summation of these probabilities to a cluster multiplied by bandwidth availabilities at this cluster is higher than this summation multiplied by a dynamic threshold. This threshold is increased if HOFR is high and vice versa. However, handovers are prioritized over new calls by not subjecting their admission decisions to this threshold. Finally, and after admitting a new call or a handover, a bandwidth proportional to the derived handover probabilities is reserved in the remaining cells of the cluster.

The work in [27] is the only CAC-SO scheme surveyed that prioritizes handovers over new calls while still differentiating between real-time and non-real-time calls. To begin with real-time services, new calls are admitted only if the desired amount of bandwidth is available at the target cell and its neighbours, whereas handovers are prioritized by being satisfied with only the minimum bandwidth. For non-real-time services, new calls are admitted by only having the desired amount of bandwidth at the target cell, whereas handovers are prioritized by being satisfied with any remaining bandwidth. Therefore, there is no need for reserving bandwidth at neighbouring cells when dealing with non-real-time calls. In all cases, the reserved bandwidth pool is increased if HOFR is high and vice versa.

3.3.2. Representative Scheme

Surveyed CAC-SO schemes are summarized as shown in Table 2 and the scheme proposed by [24] is chosen as our CAC-SO representative scheme for the following reasons:

- It is based on the most commonly used dynamic guard channel policy which prioritizes handovers over new calls,
- It monitors the locally processed HOFR and therefore no signalling is needed.

Algorithm 2 shows the pseudocode. However, we have modified the scheme, as shown in lines 6-10 and 15-20, to account for the mobile operator's CBP threshold and to allow for adjustable mobile operator thresholds. The scheme

Table 2: CAC Self-optimization Schemes Summary.

Scheme	Control Parameters	Technique	SON Architecture
S. Jeong et al. [23] scheme.	CAC guard channel policy dynamic threshold	Adjustments are made in response to the packet drop rate. The goal is to avoid real-time calls dominance.	Distributed
Y. Zhang et al. [24] scheme.		Adjustments are made in response to HOFR only. The goal is to prioritize handovers over new calls.	
K. Spaey et al. [25] scheme.		Adjustments are made in response to HOFR, CBP and the fraction of calls with a low throughput. The goal is to prioritize handovers over new calls.	
F. Yu et al. [26] scheme.		Adjustments are made in response to HOFR. However, bandwidth reservations are made at cells where the derived user handover probability exceeds a certain threshold, and these reservations are proportional to these handover probabilities. The goal is to prioritize handovers over new calls.	Centralized or Hybrid
C. Oliveira et al. [27] scheme.		Adjustments are made in response to HOFR. Moreover, real-time calls are not admitted unless other bandwidth reservations are made at neighbouring cells. Non-real-time calls do not require that. This difference in treatment ensures that real-time calls do not dominate. Finally, handovers are prioritized over new calls by not requiring as much bandwidth at admission phase.	

Algorithm 2 CAC-SO Representative Scheme [24].

```
1.  Initialize HOFR_TH and CBP_TH
2.  while Cell is ON do
3.    if an optimization interval has passed then
4.      Compute optimization interval HOFR and CBP
5.      if HOFR≥α1×HOFR_TH and NHOF>0 then
6.            if CBP≤CBP_TH then
7.                Decrease CAC_TH;
8.            else
9.                CAC_TH=CAC_TH;
10.           end if
11.     end if
12.     if HOFR≤α2×HOFR_TH and NSHO≥NSHO_TH then
13.           Increase CAC_TH;
14.     end if
15.     if HOFR<HOFR_TH and CBP<CBP_TH then
16.           Decrease HOFR_TH and CBP_TH;
17.     end if
18.     if HOFR>HOFR_TH and CBP>CBP_TH then
19.           Increase HOFR_TH and CBP_TH;
20.     end if
21.   end if
22. end while
```

starts by initializing the operator KPI thresholds. Then, it periodically measures local HOFR and CBP in order to evaluate how the guard channel policy's dynamic threshold (CAC_TH) should be adjusted. The two parameters (α_1 and α_2) are used to prevent oscillations, where $\alpha_1 > \alpha_2$ and both $\alpha_1 \& \alpha_2 < 1$. Responses to high HOFR are accelerated by including the Number of Handover Failures (NHOF), whereas responses to low HOFR are slowed down by including the Number of Successful Handovers (NSHO). This gives handovers a higher priority over new calls. Most importantly, this scheme trades off HOFR with CBP.

3.4. Load Balancing Self-optimization

3.4.1. Survey of Schemes

All LB-SO schemes surveyed balance network load by controlling cell coverage areas either by adjusting transmission powers or $Q_{offsets}$. An exchange of load information between cells is always needed which generates signalling overhead.

In [28], a scheme is proposed that is based on adjusting transmission power level in response to current cell load. It starts by exchanging load information between cells. The average of these loads is compared against current cell load, if this average load is lower than current cell load, then current cell power level is decreased and vice versa. However, adjusting power might cause gaps and

overlaps. Therefore, authors develop another scheme that adjusts the minimum power level a cell can reach. This is done by monitoring CDP, and if it is high, then a gap is detected and the minimum power level is increased. The opposite applies when detecting coverage overlaps.

Authors in [29] claim that adjusting power levels risks the network with more coverage overlaps and gaps. Therefore, they propose a scheme that adjusts $Q_{offsets}$ instead. It starts with $Q_{offsets}$ set to zero. Then, cell load measurements are exchanged periodically and $Q_{offsets}$ are adjusted accordingly. $Q_{offsets}$ are increased at cells with a load lower than neighbouring cell loads and vice versa. However, if the absolute load difference is lower than a certain threshold, then no adjustment is made.

Several other schemes adjust $Q_{offsets}$. In [30], authors propose that $Q_{offsets}$ should be adjusted in response to CBP differences between different cells. This difference along with the current Q_{offset} values are used as inputs to a fuzzy logic algorithm in order to make the Q_{offset} adjustment decisions.

The authors in [31] propose a Q_{offset} adjusting scheme. The scheme is based on an autonomic flowing water balancing method inspired by the connected vessels theories in physics. With this method, each cell monitors its load, detect overload situations and adjust $Q_{offsets}$.

The work in [32] is the only LB-SO scheme surveyed that adjusts both transmission power levels and $Q_{offsets}$. Similar to [30], both of these adjustments are made using a fuzzy logic controller. For the Q_{offset} adjustments, the inputs are current $Q_{offsets}$ and cell load ratio differences, whereas outputs are the adjusted $Q_{offsets}$. For the power adjustments, the inputs are the load ratio difference, the difference between the current cell transmission power level and its default level, and another input called the ping pong parameter. The outputs are the required transmission power levels.

3.4.2. Representative Scheme

Surveyed LB-SO schemes are summarized as shown in Table 3 and the scheme proposed by [29] is chosen as our LB-SO representative scheme for the following reasons:

- It avoids causing coverage gaps and overlaps by not adjusting cell transmission powers,
- It adjusts the commonly used standardized Q_{offset} control parameters.

Algorithm 3 shows the pseudocode. This scheme starts by initializing the operator load difference threshold (Load_Diff_TH). Then, it periodically measures the serving cell load (CL_s) and the neighbouring cell loads (CL_n) in order to evaluate whether Q_{offset} should be decreased, increased or stay the same. All of these adjustments are processed locally after gathering load information from neighbouring cells. Most importantly, this scheme trades off PPHOR with CBP and HOFR.

Table 3: Load Balancing Self-optimization Schemes Summary.

Scheme	Control Parameters	Technique	SON Architecture
I. Ashraf et al. [28] scheme.	Transmission power levels	Neighbouring cell loads average is compared against current cell load to adjust cell power level. The minimum power level is adjusted based on CDP to prevent gaps and/or overlaps.	Centralized or Hybrid
R. Kwan et al. [29] scheme.	$Q_{offsets}$	$Q_{offsets}$ are adjusted in accordance with cell load differences.	
P. Muñoz et al. [30] scheme.		Neighbouring cell CBPs and $Qoffsets$ are fed to a fuzzy logic controller that decides how $Q_{offsets}$ should be adjusted.	
H. Zhang et al. [31] scheme.		The scheme is based on a method inspired by the connected vessels theories where each cell detects overloads and adjusts $Q_{offsets}$ accordingly.	
J. Aviles et al. [32] scheme.	$Q_{offsets}$ and Transmission power levels	This scheme adjusts both of $Q_{offsets}$ and transmission power levels using fuzzy logic controllers. However, the ping pong parameter should be high before allowing power levels to be adjusted and risking the network with more gaps and/or overlaps.	

Algorithm 3 LB-SO Representative Scheme [29].

1. Initialize Load_Diff_TH
2. **while** Cell is ON **do**
3. **if** an optimization interval has passed **then**
4. **for** all neighbouring cells **do**
5. Collect last optimization interval CL_n
6. **end for**
7. **for** all neighbouring cells **do**
8. **if** $CL_n - CL_s >$Load_Diff_TH **then**
9. Increase $Q_{offset_{s,n}}$;
10. **end if**
11. **if** $CL_n - CL_s <$Load_Diff_TH **then**
12. Decrease $Q_{offset_{s,n}}$;
13. **end if**
14. **if** $abs(CL_n - CL_s) \leq$Load_Diff_TH **then**
15. $Q_{offset_{s,n}} = Q_{offset_{s,n}}$;
16. **end if**
17. **end for**
18. **end if**
19. **end while**

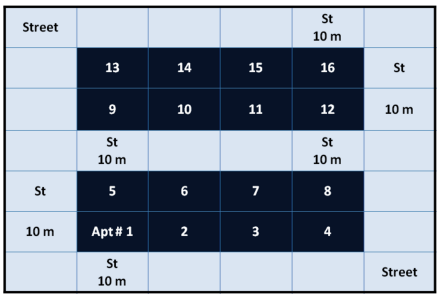

Figure 3: Network Topology.

4. Simulation Environment

4.1. Scenario

The network topology is the dual-stripe shown in Figure 3. At each apartment of the 16 shown, there is a femtocell dropped randomly. The whole dual stripe block is located at the intersection area of three macrocell sectors where the macrocellular tier coverage is expected to be limited. This weak macrocell coverage should lead UEs to rarely choose macrocells for their new call and handover requests and therefore our network performance would capture, as much as possible, the effect of schemes being studied and implemented only in the femtocellular tier. Meanwhile, macrocellular tier interference effect would still be captured. In fact, surrounding the three macrocell sectors mentioned are two rings of 3-sector macrocells to account for the macrocell tier interference affect.

Table 4: Simulation Scenario Assumptions.

Item	Assumption
Center Carrier Frequency	2 GHz
Downlink System Bandwidth	3 MHz
Macrocell Intersite Distance	1732 metres
Macrocell DL TX Power Level	43 dBm
Maximum Femtocell DL TX Power Level	20 dBm
Indoor Users mobility model	Random Walk Mobility Model with Bouncing Back
5 Vehicles Speed	30 km/h
Initial barring Timer value	15 seconds
UE Class's Peak Data Rate	10 Mbps
Minimum acceptable SINR level	-10 dB
UE Receiver Sensitivity	-110 dBm

Both indoor and vehicular outdoor users are assumed in the dual stripe block. A fixed load is assumed for macrocells including outside the dual stripe block. This fixed load assumption is made to ensure including macrocellular tier interference. We have verified in the upcoming Section 5 that varying macrocellular tier load has no effect on final results. We attribute this to the weak signal and interference received by indoor and outdoor UEs from these distant macrocells and therefore these macrocells are rarely chosen while having minor interference effect reaching femtocells located at the dual stripe block.

Within 5 seconds of simulation time, each user starts sending a new call request. No mobility-based scaling factors are assumed and the same standardized cell barring technique is assumed for handover failures. The adoption of this barring technique is based on the fact that rejected handover requests would most probably be rejected anyway if they were sent to the same target cell within a short time after the first handover failure.

In order to comply with NGMN recommendations [33], we have adopted the traffic mix: 30% VoIP, 20% interactive Gaming, 20% Near Real-Time Video Streaming, 20% HTTP and 10% FTP service. For VoIP, Gaming and Near-Real-Time Video Streaming services, active and idle call durations are drawn from exponential distributions. Whereas, both HTTP and FTP services are assumed to be continuously downloading webpages and files after finishing the reading of a previous one. Most importantly, every user sticks to the same single service type throughout the entire simulation time. Table 4 and 5 summarize main simulation scenario assumptions and call duration means, respectively.

4.2. Simulator Structure

Our MATLAB-written discrete event simulator structure is shown in Figure 4. It is composed of nine modules where unidirectional arrows show that some modules just receive/send from/to others while bidirectional arrows show

Table 5: Active & Idle Call Duration Means.

Service Type	Active Call Duration Mean	Idle Duration Mean
VoIP	5 minutes	5 minutes
Gaming	10 minutes	5 minutes
Near Real-Time Video Streaming	20 minutes	5 minutes

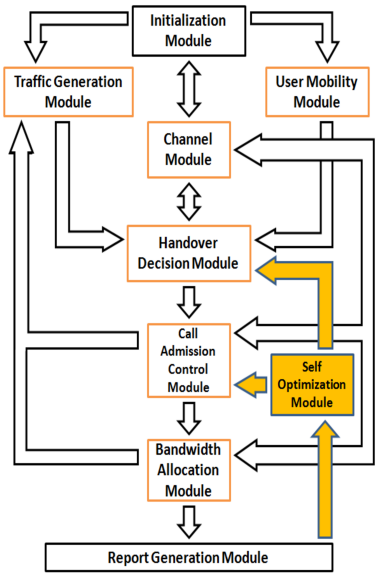

Figure 4: Simulator Overall Structure.

mutual exchanges of information. The goal is to simulate the standardized LTE handover procedure while allowing us to study interactions between the handover-related self-optimization use cases of interest.

The **Initialization Module** initializes **User Mobility Module** and **Traffic Generation Module** to start generating users' mobility and traffic events, respectively. The **Initialization Module** interacts with **Channel Module** when computing initial femtocell power levels since this **Channel Module** provides shadow fading and SINR values needed by all other modules.

The **Handover Decision Module** represents the handover decision functionality at the source cell and reacts to both user mobility and traffic events. To make handover decisions, this module consults **Channel Module** for neighbouring cells RSRP measurements . These decisions are sent afterwards to **Call Admission Control Module** which represents the CAC functionality at the target cell. Based on current target cell load and initial bandwidth reservations made by **Channel Module**, these decisions may get rejected which can cause call blocks or drops. **Traffic Generation Module** needs to get updated of

such events to bring users back into the system.

For granted handovers and new calls, we have assumed a fixed core network signalling delay. After this delay, final bandwidth allocations are made by **Bandwidth Allocation Module** based on **Channel Module** bandwidth estimations. Therefore, **Bandwidth Allocation Module** may find that some calls have low bandwidth and can no longer be sustained. Again, **Traffic Generation Module** needs to get updated of such call drop events.

Finally, **Handover Decision Module** is responsible for handover decisions through its Q_{Hyst}, TReselection and Q_{offset} control parameters. Whereas, **Call Admission Control Module** is responsible for admission decisions through its conventional guard channel policy threshold. With the introduction of **Self-optimization Module**, these control parameters are adjusted in response to KPI changes as detected, collected and sent by **Report Generation Module**. The **Report Generation Module** outputs final results and enables real time monitoring. Next, we go through each module in brief while further details can be found in our thesis work in [34].

4.2.1. Initialization Module

This module initializes user and access point states. It also sets femtocells' downlink transmission power levels based on the measurement based method followed by [35]. However, thermal noise, shadow fading, all interfering macrocell and femtocell signals are considered this time. The objective is to achieve a zero-dB SINR at the apartment edge. Indeed, this is done by interacting with Channel Module.

4.2.2. Channel Module

Based on the Small Cell Forum SINR computation assumptions [36] summarized in Table 6, this module provides other modules with RSRP and SINR measurements needed after computing shadow fading maps. These maps are generated according to the correlation matrix based method followed in [37]. Afterwards, they are used to compute the auto-correlated shadow fading values. With these shadow fading values, we have:

$$RSRP_{SC2UE} = P_t - 10\log_{10}(N_{AS}) + G_{Cell} + A(\theta) - PL - SF + G_{UE}{}^{1}$$

$$RSRP_{IC2UE} = P_t - 10\log_{10}(N_{AS}) + 10\log_{10}(L_I) + G_{Cell} + A(\theta) - PL - SF + G_{UE}{}^{2}$$

$$N_{thermal} = -174 + 10\log_{10}(\triangle f) + N_F$$

$$SINR_{Sub} = RSRP_{SC2UE} - (N_{thermal} + 10\log_{10}(\sum_{i=1}^{N_{IC}} 10^{RSRP_{IC_i2UE}/10}))$$

[1] We do not account for SF if $R < 1m$.

[2] If $L_I = 0$, then $RSRP_{IC2UE}$ coming from this cell should be ignored.

Table 6: SINR Computation Assumptions.

Item	Assumption
Macrocell Antenna Type	3-sector antenna
Macrocell Antenna Bore-sight	It points towards flat side of the cell
Macrocell Antenna Azimuth Pattern (dB)	$A(\theta) = -min\left[12\left(\frac{\theta}{70}\right)^2, 20\right]$ where $-180 \leq \theta \leq 180$
TX-RX Separation Distance (metre)	R
Distance inside the house (metre)	$d_{2D,indoor}$
Outdoor UE to Macrocell Path Loss (dB)	$PL = 15.3 + 37.6 \log_{10} R$
Indoor UE to Macrocell Path Loss (dB)	$PL = 15.3 + 37.6 \log_{10} R + 10$
Macrocell Antenna Gain including the Cable Loss (dBi)	$G_{Cell}(macro) = 14$ dBi
Femtocell Antenna Type	Omnidirectional
Femtocell Antenna Azimuth Pattern (dB)	$A(\theta) = 0$
UE to Femtocell Path Loss (dB)	$PL = 127 + 30 \log_{10}(\frac{R}{1000})$
Path Loss if $R < 1m$ (No shadowing) (dB)	$PL = 38.46 + 20 \log_{10} R + 0.7 d_{2D,indoor}$
Femtocell Antenna Gain including the Cable Loss (dBi)	$G_{Cell}(femto) = 5$ dBi
User Antenna Gain including the Cable Loss (dBi)	$G_{UE} = 0$ dBi
Thermal Noise Density (dBm/Hz)	-174 dBm/Hz
Subcarrier Frequency Spacing (kHz)	$\triangle f = 15$ kHz
UE Noise Figure (dB)	$N_F = 9$ dB

Where:

$RSRP_{SC2UE}$	is the Serving Cell RSRP received per UE subcarrier in dBm.
P_t	is the total cell transmitted power in dBm.
N_{AS}	is the serving cell number of Active Subcarriers.
SF	is the auto-correlated Shadow Fading value in dB.
$RSRP_{IC2UE}$	is the Interfering Cell RSRP received per UE subcarrier in dBm.
L_I	is the Interfering cell load which could vary from 0 to 1 for a fully loaded cell.
$N_{thermal}$	in the thermal Noise in dB.
$SINR_{Sub}$	is the user's SINR measurement per UE Subcarrier in dB.
N_{IC}	is the number of Interfering Cells, where all cells are considered in the interference computation.

As it can be seen from the above equations, we assume no fast fading similar to [38]. In addition, and similar to [39], a flat power spectral density is assumed which means that power allocated for each subcarrier equals the total cell's transmission power divided by the number of active subcarriers. Finally, we assume that intra-cell interference is eliminated and that inter-cell interference depends on the interfering cell loads which can be used as an indication for the

probability of causing interference. This simplified method of computing the inter-cell interference is adopted by several authors including [40, 41, 42].

4.2.3. User Mobility Module

This module generates mobility events of both indoor and vehiclular users. Indoor users move according to a random walk mobility model, whereas vehicles move in a predefined path with a fixed speed. All user locations are set initially by the Initialization Module and then gets sent to other modules as needed.

4.2.4. Traffic Generation Module

In what follows, we briefly explain the five traffic sources adopted according to [37], their call dropping and blocking criteria:

VoIP

During a voice call there are active and inactive periods. Both are modeled with exponential distributions of a 1.25 second mean. We simulate the active period as a 16 kbps Constant Bit Rate (CBR) service, whereas the inactive period is assumed to be completely silent. Our assumption of a 16 kbps CBR came from the 12.2 kbps adaptive multi-rate voice encoding scheme adopted with the link adaptation disabled, and from assuming that for every 320 bits of voice packets there is a payload of only 244 bits. In fact, disabling link adaptation and using the full rate of 12.2 kbps captures the channel's worst case scenario. For the dropping and blocking criteria, we assume that a VoIP call is blocked or dropped if at any point in time there are no sufficient resources to provide the 16 kbps throughput required.

Interactive Gaming

Similar to voice, interactive gaming is a real-time service. The first downlink Gaming packet starts, with a random uniform distribution, within the first 40 msec of starting the call. Since the average downlink Gaming packet size is 380 bytes, including the 2-byte User Datagram Protocol (UDP) header, and the average downlink packet arrival time is 52 msec, we assume a CBR service of 57 kbps throughput. These average values are decided after considering about 1 million samples of packet sizes and packet arrival times according to the distributions given in [37]. Similar to VoIP calls, we assume that a Gaming session is blocked or dropped if at any point in time there are no sufficient resources to provide the 57 kbps throughput required.

Near Real-Time Video Streaming

To simulate the video streaming packet behaviour, we follow the 8 packets per 100 msec frame rule and the packet or "slice" size's Truncated Pareto distribution with 100-byte mean and the maximum packet size of 250 bytes. Moreover, the additional 4-byte RTP/UDP/IP header is also considered.

At the beginning of the simulation, we assume that the user's video playout buffer is full with the video streaming bits necessary for a dejittered 64 kbps

video streaming service for the next 5 seconds. In order to prevent the user's video playout buffer from getting dry due to the 64 kbps video streaming service at the user side, we need to provide this user buffer with the accumulated streaming video bits scheduled at the base station buffer in a near-real-time fashion. This also prevents the base station scheduler buffer, which also has a 5-second dejittering window, from getting into overflow. Otherwise, the Video Streaming user is considered in outage.

HTTP

Each webpage has a main object and several embedded objects. After downloading the main object, a parsing time is needed. Following that, the downloading of the embedded objects will start, and when it ends the webpage will be ready for viewing.

According to [37], main objects are modeled by a lognormally distributed size with a mean of 10710 bytes and a standard deviation of 25032 bytes. This distribution is truncated at the minimum value of 100 bytes and the maximum value of 2 Mbytes. The time needed to parse this main object follows an exponential distribution with a mean of 0.13 second.

For the embedded objects, each object is modeled by a lognormally distributed size with a mean of 7758 bytes and a standard deviation of 126168 bytes. This distribution is truncated at the minimum value of 50 bytes and the maximum value of 2 Mbytes. The number of these embedded objects follows a truncated Pareto distribution with a mean of 5.64 and a maximum value of 53.

All of the above mentioned object sizes need to be adjusted to account for the one 40-byte IP header in each Maximum Transmission Unit (MTU), where the size of a single MTU is found to be 1500 bytes in 76% of the packets and 576 bytes in 24% of the packets. More importantly, this MTU size is fixed between all the different object types in each single webpage. The time needed to read the webpage, after downloading all of these different objects, follows an exponential distribution with a mean of 30 seconds. Finally, an HTTP user is considered in outage if the average service throughput is less than the minimum required throughput of 128 kbps.

FTP

According to the FTP evaluation methodology given in [37], the file size is lognormally distributed with a mean of 2 Mbytes and a standard deviation of 0.722 Mbytes. This distribution is truncated at the maximum value of 5 Mbytes. Similar to HTTP, the file size is adjusted to account for the one 40-byte IP header in each MTU, where the size of a single MTU is found to be 1500 bytes in 76% of the packets and 576 bytes in 24% of the packets. The reading time of this file size follows an exponential distribution with a mean of 180 seconds. Finally and similar to HTTP users, an FTP user is considered in outage if the average service throughput is less than the minimum required throughput of 128 kbps.

4.2.5. Handover Decision Module

This module executes UE neighbourhood discovery scanning by interacting with the Channel Module. A user's call is dropped or blocked if no detectable cell is found. After the neighbourhood discovery, this module makes handover decisions based on received UE RSRP list and current source cell's Q_{Hyst}, TRe-selection and $Q_{offsets}$.

4.2.6. Call Admission Control Module

After interacting with the Channel Module and based on current target cell load and bandwidth reservations made, the target cell decides whether to admit a request or not. This can be done by adopting the conventional guard channel policy. If a handover request is granted, then this initiates handover execution and completion phases. Otherwise we have either a handover failure or just a call block where both cases initiate a barring timer. In all cases, we assume that no bandwidth allocation yields more than 10 Mbps and less than -10 dB SINR. According to [36], the throughput can be estimated using the attenuated and truncated Shannon's Capacity formula. When using this formula, the attenuation, or as it is sometimes called, the Correction Factor [43], is considered to account for the inherent implementation losses, including the Cyclic Prefix (CP) Loss and the Reference Symbol Loss as explained in [43]. Therefore, and assuming the LTE OFDMA RAT, Shannon's capacity formula becomes:

$$Throughput_{total} = F \times B \times \log_2(1 + 10^{SINR_{sub}/10})$$

and:

$$F = CyclicPrefixLoss \times ReferenceSymbolLoss$$

$$CyclicPrefixLoss = \frac{T_{frame} - T_{CP}}{T_{frame}}$$

$$ReferenceSymbolLoss = \frac{N_{SC} \times N_S/2 - 4}{N_{SC} \times N_S/2}$$

$$B = \frac{N_{SC} \times N_S \times N_{rb}}{T_{sub}}$$

Where:

$Throughput_{total}$	is the total throughput received by the user in bps.
F	is the attenuation or the Correction Factor.
B	is the bandwidth allocated to the user in Hz.
T_{frame}	is the duration of one OFDMA frame (= 10 msec) .
T_{CP}	is the total CP time of all the OFDMA symbols within one frame, which equals: $(5.2\mu sec + 6 \times 4.69\mu sec) \times 20 = 666.8\mu sec$.
N_{SC}	is the number of subcarriers in one Physical Resource Block (PRB), which equals 12 subcarriers.

N_S is the number of OFDMA symbols in one subframe, which equals 14 symbols assuming that the normal CP is set.

N_{rb} is the number of PRBs allocated to the user, where each PRB has a bandwidth of 180 kHz that can only be used by one user; i.e., it is the smallest bandwidth unit that can be allocated.

T_{sub} is the duration of one OFDMA subframe (= 1 msec).

After having the target cell granting a handover request or a new call request, we assume accordingly a constant delay.

4.2.7. Bandwidth Allocation Module

After interacting with the Channel Module, this module allocates final resources for handover and new call requests. It monitors call statuses to check if some calls meet the dropping criteria explained previously in the Traffic Generation Module, or if some calls have a low SINR level. Notice that throughputs are estimated using Shannon's Capacity formula.

4.2.8. Self-optimization Module

This module is where all of our femtocell self-optimization schemes are implemented and studied. It is fed by the Report Generation Module with needed KPIs in order to adjust accordingly the fixed control parameters of both the Handover Decision Module and the Call Admission Control Module.

4.2.9. Report Generation Module

This module provides the user interface throughout the entire simulation time. This interface shows remaining simulation time, individual cell loads and all KPI statistics of interest. This module can also produce an AVI video file for the entire simulation time, user traces and cell traces for validation purposes.

5. Experiments

As mentioned previously in Section 4, we have first proven that no effect takes place when varying macrocellular tier load. Then representative schemes are validated followed by experimenting their mutual interactions. The following abbreviations are used throughout upcoming experiments:

- **HOCAC-SO:** stands for the interaction between HO-SO and CAC-SO schemes.
- **HOLB-SO:** stands for the interaction between HO-SO and LB-SO schemes.
- **CACLB-SO:** stands for the interaction between CAC-SO and LB-SO schemes.
- **HOCACLB-SO:** stands for the interaction between all representative schemes; i.e. HO-SO, CAC-SO and LB-SO schemes.

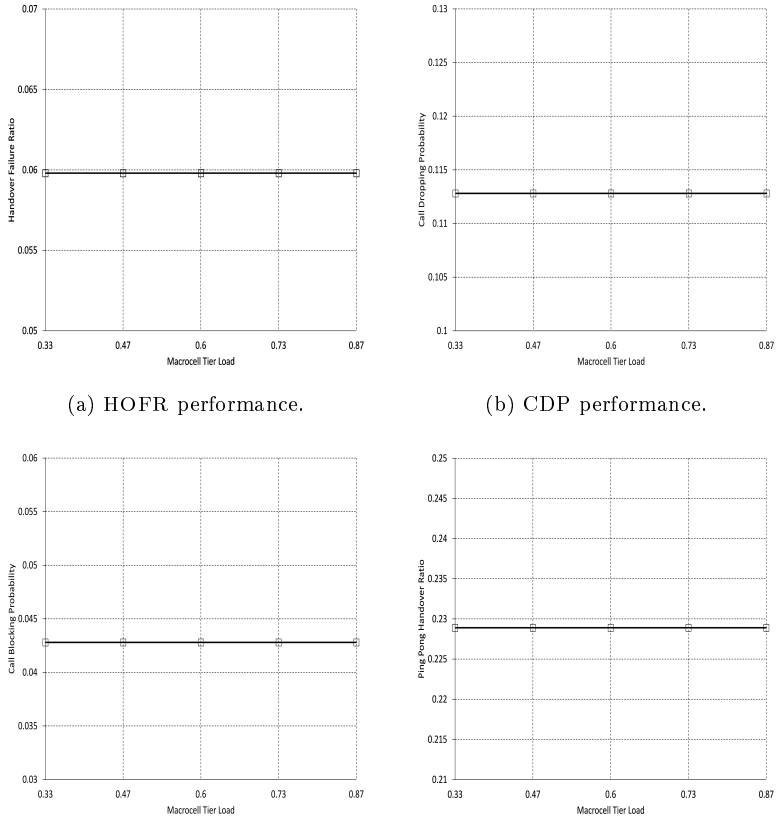

(a) HOFR performance.

(b) CDP performance.

(c) CBP performance.

(d) PPHOR performance.

Figure 5: KPIs against macrocellular tier load.

5.1. Macrocellular Tier Load Effect

In this experiment, the macrocellular tier load is varied while adopting the same static control parameter setting. Figure 5 shows that almost no effect takes place in terms of HOFR, CDP, CBP and PPHOR. We attribute this to the fact that users rarely choose macrocells due to their weak signal.

5.2. Individual Scheme Experiments

Figure 6 shows representative schemes performance in terms of HOFR, CDP, CBP and PPHOR. We notice that in femtocell environments, PPHOR is high which leads the HO-SO scheme to aggressively increase its Q_{Hyst} and TReselection parameters while decreasing the number of outbound handovers, PPHOR and HOFR. However, this leads these outbound handovers to be locked to a femtocell that has a signal strength that is lower than its neighbours which

eventually leads to call drops, an increased CDP, a less utilization and therefore a less CBP.

We also notice that CAC-SO scheme prioritizes handovers over new calls which leads to more new call blocks, less handover failures and therefore less call drops. Less call drops are due to the fact that users are getting their handover requests granted. However, this scheme does not clearly differentiate between normal and ping pong handovers, which means no clear effect on PPHOR.

Finally, LB-SO scheme always tries to balance the load as soon as it discovers a tangible load difference. This balancing enhances the chances for new calls and handovers of finding bandwidth which decreases both HOFR and CBP while increasing PPHOR. However, and since the main cell selection/reselection criterion is based on choosing the cell with the highest signal strength, most of the overutilized cells would be the cells with the highest downlink transmission power levels and vice versa. Therefore, this load balancing technique forces users to leave the higher power overutilized cells to the lower power underutilized cells which means a higher interference for these users and as a result an increased CDP.

5.3. Interaction Experiments

5.3.1. HOCAC-SO schemes interaction

Figure 7 shows this performance interaction in terms of HOFR, CDP, CBP and PPHOR. We find that the CAC-SO scheme at the target femtocell guards some resources to the handover requests initiated by the HO-SO scheme at the source femtocell. This makes the CAC-SO scheme share the burden of decreasing HOFR with the HO-SO scheme and overall we have an even less HOFR. The HO-SO scheme is now using a bit smaller Q_{Hyst} and TReselection parameters and therefore we have a slight CDP decrease but a slight PPHOR increase. In addition, the CAC-SO scheme now neither needs to reserve as many resources for handovers nor block as many new calls. Therefore, the system experiences a slight CBP decrease.

5.3.2. HOLB-SO schemes interaction

Figure 8 shows this performance interaction in terms of HOFR, CDP, CBP and PPHOR. The HO-SO scheme attempts to limit the number of outbound handovers in order to decrease HOFR. This strategy contradicts the LB-SO scheme strategy and therefore leads the LB-SO to perform sub-optimally in terms of decreasing HOFR and CBP. However, the HO-SO scheme is now observing less HOFR, with the help of the LB-SO scheme, which leads to smaller HO-SO control parameters. This causes a slight CDP decrease and a slight PPHOR increase. In fact, PPHOR is still much lower than what it used to be when the LB-SO scheme was operating separately due to the HO-SO scheme effect.

5.3.3. CACLB-SO schemes interaction

Figure 9 shows this performance interaction in terms of HOFR, CDP, CBP and PPHOR. The LB-SO scheme has found channels for its outbound handover

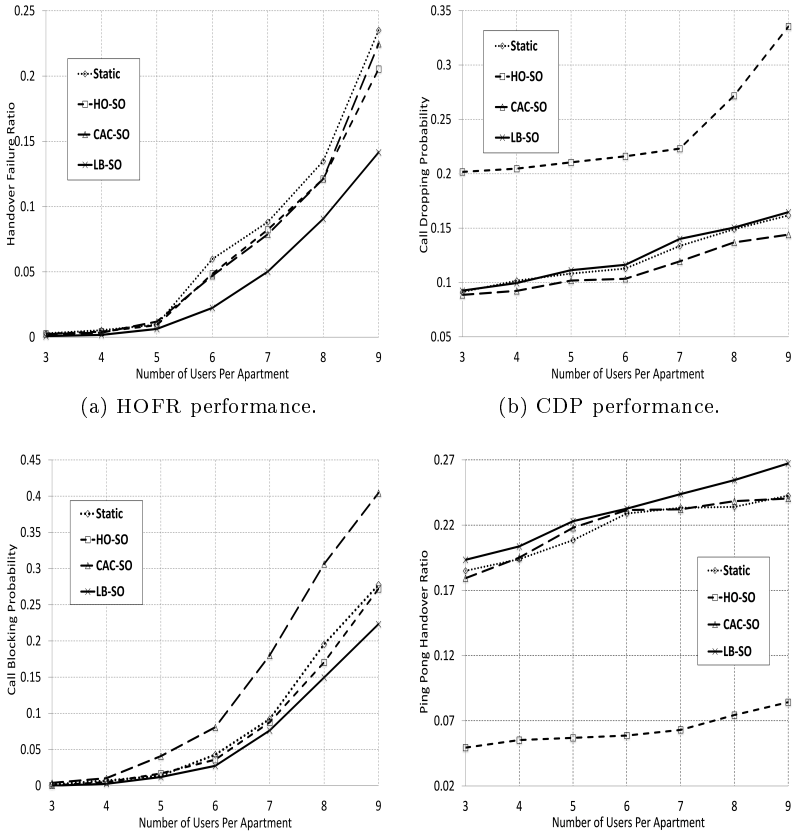

(a) HOFR performance.

(b) CDP performance.

(c) CBP performance.

(d) PPHOR performance.

Figure 6: Representative schemes KPIs against number of users.

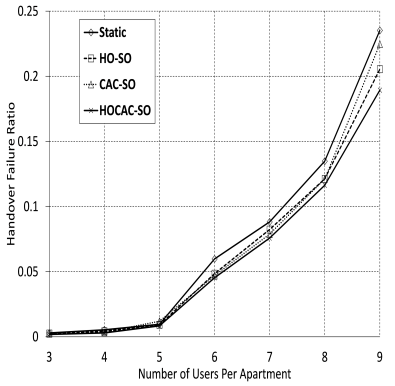

(a) HOFR performance.

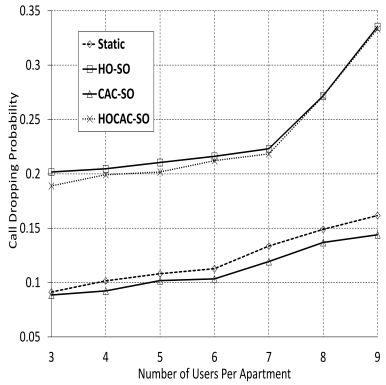

(b) CDP performance.

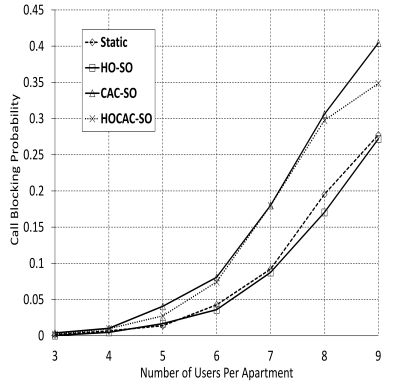

(c) CBP performance.

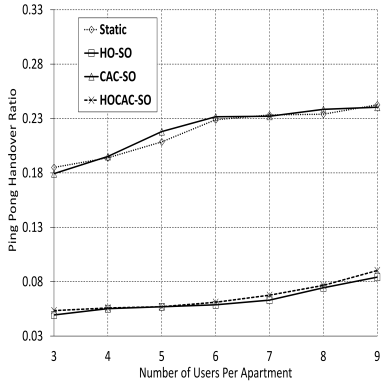

(d) PPHOR performance.

Figure 7: HOCAC-SO interaction KPIs against number of users.

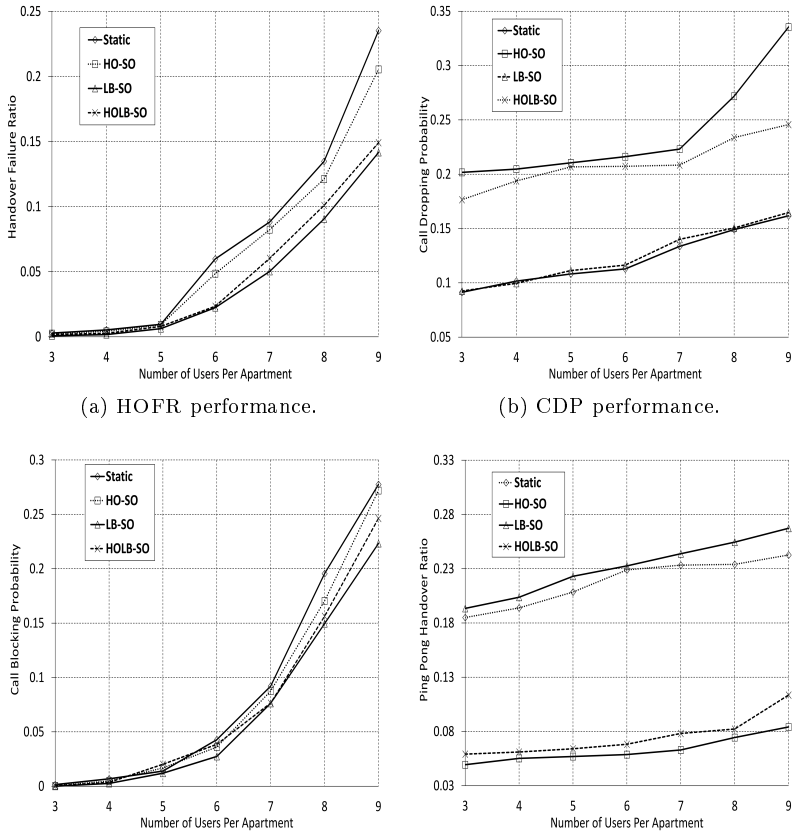

(a) HOFR performance.

(b) CDP performance.

(c) CBP performance.

(d) PPHOR performance.

Figure 8: HOLB-SO interaction KPIs against number of users.

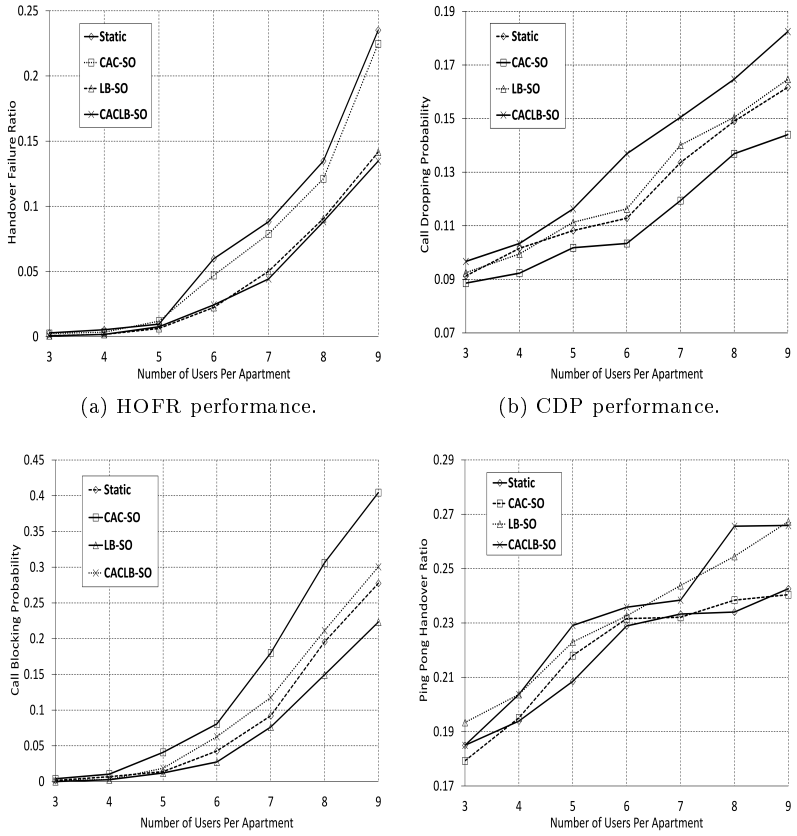

(a) HOFR performance.

(b) CDP performance.

(c) CBP performance.

(d) PPHOR performance.

Figure 9: CACLB-SO interaction KPIs against number of users.

decisions reserved by the CAC-SO scheme at the target cells, which results in further decreasing HOFR. This in fact has spoiled the LB-SO scheme by allowing it to initiate even more handovers from the overutilized high power cells towards the underutilized low power cells, and therefore causing more call drops. However, the CAC-SO scheme is no longer blocking as many new calls as it used to do before. But since the CAC-SO scheme is still taking part in the process of decreasing HOFR, the CAC-SO scheme is still causing a high CBP. For the PPHOR, the LB-SO scheme still causes a high PPHOR. However, no clear interaction effect is observed in terms of PPHOR.

5.3.4. HOCACLB-SO schemes interaction

Figure 10 shows our HOCACLB-SO interaction results in terms of HOFR, CDP, CBP and PPHOR. In what follows we discuss these results:

Effects of adding LB-SO to HOCAC-SO:

Introducing LB-SO scheme into HOCAC-SO interaction lowers HOFR. From earlier experiments, we have noticed that LB-SO scheme cooperates positively with both HO-SO and CAC-SO schemes in terms of decreasing HOFR. Although, LB-SO scheme has not taken its full potential after interacting with HO-SO scheme. Further decrease in HOFR leads HO-SO scheme to use lower control parameters which results in more outbound handovers and a higher PPHOR. However, interacting with CAC-SO scheme has almost no clear PPHOR effect.

LB-SO scheme provides a mixed interaction result when it is introduced with the HOCAC-SO interaction in terms of CDP; LB-SO scheme should increase CDP after interacting with CAC-SO scheme but decrease CDP after interacting with HO-SO scheme. Interestingly, the HOLB-SO interaction CDP decrease dominates and causes a lower CDP. This should be attributed to the fact that introducing LB-SO scheme into HOCAC-SO interaction would lead LB-SO scheme to decrease the number of handover failures even further and therefore causes HO-SO scheme to relax and cause even less call drops. Finally, introducing LB-SO scheme into HOCAC-SO interaction causes clearly even lower call blocks.

Effects of adding CAC-SO to HOLB-SO:

Introducing CAC-SO scheme into HOLB-SO interaction leads to a lower HOFR since CAC-SO scheme interacts positively with both HO-SO and LB-SO schemes in terms of decreasing HOFR. However, CAC-SO scheme increases CDP of the HOLB-SO interaction since CAC-SO scheme increases CDP to a larger extent, after interacting with LB-SO scheme, than decreasing CDP after interacting with HO-SO scheme. Finally, CAC-SO scheme definitely increases CBP, while almost making no major PPHOR change.

Effects of adding HO-SO to CACLB-SO:

Introducing HO-SO scheme into CACLB-SO interaction limits LB-SO scheme's ability in terms of decreasing HOFR and CBP. Therefore, both of these KPIs slightly increase despite the fact that HO-SO and CAC-SO schemes cooperate in achieving a lower HOFR. Moreover, introducing HO-SO scheme also increases CDP. In fact, introducing HO-SO scheme always increases global CDP. This drawback comes with the advantage of a decreased PPHOR.

6. Discussion

We begin our discussion by summarizing previously observed advantages and disadvantages introduced in LTE femtocell environments by each scheme and interaction as shown in Table 7 and Table 8, respectively. While classifying a certain interaction outcome as an advantage or a disadvantage, we compare this outcome against its counterpart in the static setting.

In Table 9, we give the performances of the different schemes and interactions a ranking (in terms of a set of signed and sequenced integer numbers). Positive

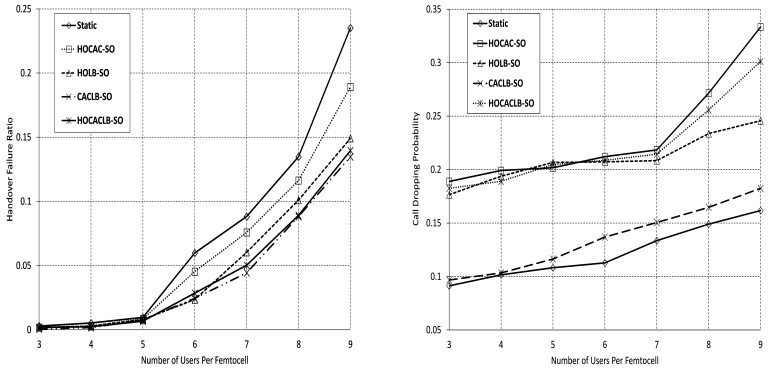

(a) HOFR performance.

(b) CDP performance.

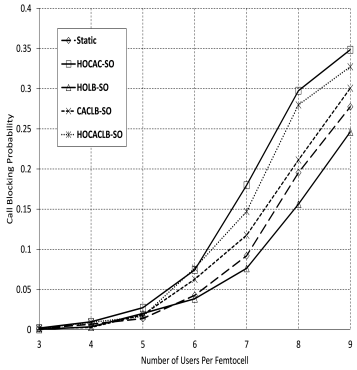

(c) CBP performance.

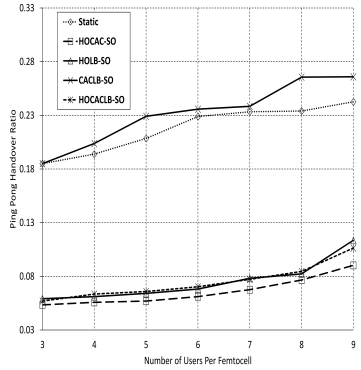

(d) PPHOR performance.

Figure 10: HOCACLB-SO interaction KPIs against number of users.

Table 7: Scheme Advantages and Disadvantages.

Scheme	Advantages	Disadvantages
HO-SO	With mostly higher Q_{Hyst} and TReselection, we have a lower HOFR and a lower PPHOR.	With mostly higher Q_{Hyst} and TReselection, we have a higher CDP and therefore a lower CBP.
CAC-SO	With channel reservations, we have a lower HOFR and therefore a lower CDP.	With channel reservations, we have a higher CBP. But no differentiation between handover types and therefore no clear effect on PPHOR.
LB-SO	With a balanced load, we have a lower HOFR and a lower CBP.	With more forced handovers, we have a higher CDP and a higher PPHOR.

Table 8: Interaction Advantages and Disadvantages.

Interaction	Advantages	Disadvantages
HOCAC-SO	CAC-SO reserves channels for the fewer number of handovers initiated by HO-SO and therefore we have an even lower HOFR. PPHOR still decreases but with CAC-SO, HO-SO is relieved and therefore less active in lowering PPHOR compared to the case when it is operating alone.	HO-SO still causes a higher CDP, but due to the CAC-SO relief, lower CDP is achieved. CAC-SO still causes high CBP, but due to the HO-SO relief, lower CBP is achieved.
HOLB-SO	LB-SO still decreases HOFR and CBP but to a lesser degree, due to the HO-SO restriction. HO-SO still decreases PPHOR but to a lesser degree, due to the LB-SO relief.	HO-SO still increases CDP but to a lesser degree, due to the LB-SO relief.
CACLB-SO	CAC-SO reserves channels for the handovers initiated by LB-SO and therefore we have an even lower HOFR.	LB-SO finds more channels reserved for its forced handovers which causes an even higher CDP. CAC-SO still increases CBP, but to a lesser degree, due to the LB-SO relief. LB-SO still increases PPHOR with CAC-SO having no clear effect.
HOCACLB-SO	Still decreases HOFR more than any other interaction except for CACLB-SO due to having HO-SO restricting LB-SO. Still decreases PPHOR as much as what HOLB-SO does, since CAC-SO does not have a clear effect on PPHOR. In addition, PPHOR is now decreased but still higher than what HOCAC-SO does due to LB-SO.	CDP and CBP are higher than any other interaction except for HOCAC-SO, due to LB-SO.

Table 9: Comparing Schemes and Interactions.

KPI	HO -SO	CAC -SO	LB -SO	HOCAC -SO	HOLB -SO	CACLB -SO	HOCACLB -SO
HOFR	-1	-1	-4	-2	-3	**-5**	-4
CDP	+6	**-1**	+1	+5	+3	+2	+4
CBP	-1	+4	**-3**	+3	-2	+1	+2
PPHOR	**-3**	0	+1	-2	-1	+1	-1

numbers indicate a KPI increase in comparison to the static setting, while the opposite holds true for the negative numbers. The sequence of these numbers indicate the relative performance of a certain KPI against its counterparts from the other schemes and interactions. A "zero" means that there is no clear effect demonstrated. The large bolded numbers in the table indicate the schemes or the interactions at which each KPI performance is the lowest or the most desired among its counterparts.

From the comparisons made in Table 9, we deduce that if we are merely interested in achieving the lowest value for each KPI *independent* from its accompanying values of the other KPIs, then the following guidelines can be recommended:

- To decrease HOFR, both of CAC-SO and LB-SO schemes should operate simultaneously, while HO-SO scheme should be disabled. This is due to the fact that, even though all of the handover-related self-optimization schemes under study caused HOFR to decrease when separate, introducing HO-SO scheme with the LB-SO scheme limits LB-SO scheme's potential in decreasing HOFR. In fact, this LB-SO scheme restriction imposed by HO-SO scheme negates the slight advantage introduced by HO-SO scheme when it interacts with CAC-SO scheme.

- To decrease CDP, HO-SO and LB-SO schemes should be disabled. CAC-SO scheme only should be enabled, since it is the only scheme that decreases CDP.

- To decrease CBP, HO-SO and CAC-SO schemes should be disabled and LB-SO scheme only should be enabled. HO-SO scheme is disabled to avoid restricting LB-SO scheme from giving its full potential in terms of decreasing CBP. For the CBP decrease introduced by HO-SO scheme, this decrease is in fact a side effect of the CDP increase introduced by the HO-SO scheme which should be avoided at all costs.

- To decrease PPHOR, HO-SO scheme only should be enabled while disabling other schemes. This is because LB-SO scheme increases PPHOR, while CAC-SO scheme aids HO-SO scheme and causes it to use even lower control parameter values which triggers more ping pong handovers.

We believe that following this list of actions would help in designing better coordination policies between the interacting HO-SO, CAC-SO and LB-SO use

cases, especially in LTE femtocell environments where a large number of handovers takes place.

7. Conclusion and Future Work

One way to enable LTE technology is to deploy femtocells at large. These femtocells have control parameters to be adjusted in order to meet certain KPI objectives. Adjusting these control parameters quickly and automatically can only be made through self-optimization use case implementations. However, these use cases might be operating simultaneously while affecting same control parameters or monitoring related KPIs; this can induce positive or negative interactions. In this study, we have shown a lack of interaction studies conducted so far in LTE femtocell environments between three handover-related self-optimization use cases, namely: handover self-optimization, call admission control self-optimization and load balancing self-optimization. All of these three use cases affect the same LTE femtocell handover procedure but through different lenses.

Our study approach was to conduct a thorough survey of proposed handover-related self-optimization schemes in order to identify three representative schemes. These representative schemes were taken afterwards throughout our interaction experiments. All of these experiments were conducted using our own in-house built, MATLAB-written and LTE complaint simulation environment. This environment was made specifically to reflect the standard LTE femtocell handover procedure in a modular way; this was explained in details throughout the paper.

Experiments revealed how interactions behave between the three handover-related self-optimization use cases. A set of recommendations were made which we believe can help designers approach better coordination policies.

For our future work, we plan to extend our study to include other handover-related self-optimization use cases (e.g. neighbour cell list self-optimization use case and coverage self-optimization use case). This would lead us to extend our simulation environment even further by including other modules. The outcome should be a broader view of how interactions behave and of how better coordination policies should be designed between interacting handover-related self-optimization use cases in LTE femtocell networks.

Finally, our simulation environment could also be extended to the LTE-Advanced technology and enhanced by adopting the more realistic mobility traces generated by the open source Simulation of Urban Mobility (SUMO) package [44]. Plans are underway to make the final enhanced LTE femtocell simulation environment accessible online for the research community at large.

8. Acknowledgments

K. Suleiman would like to acknowledge the support of the Libyan Ministry of Higher Education and Scientific Research. The authors would also like to acknowledge the support and funding of the National Science and Engineering Research Council of Canada (NSERC).

References

[1] V. Chandrasekhar, J. Andrews and A. Gatherer. "Femtocell networks: a survey." *IEEE Communications Magazine,* vol. 46, no. 9, pp. 59-67, Sep. 2008. http://dx.doi.org/10.1109/MCOM.2008.4623708.

[2] S. R. Hall, A. W. Jeffries, S. E. Avis and D. D. N. Bevan. "Performance of Open Access Femtocells in 4G Macrocellular Networks," presented at the Wireless World Research Forum 20 (WWRF 20), Ottawa, Canada, 2008.

[3] ABI Research. "High Inventory and Low Burn Rate Stalls Femtocell Market in 2012." Internet: http://www.abiresearch.com/press, Jul. 5, 2012 [Nov. 13, 2012].

[4] K. Suleiman, A. M. Taha and H. Hassanein. "Standard-Compliant Simulation for Self-Organization Schemes in LTE Femtocells," in *IEEE 39th Local Computer Networks Conference (LCN),* 2014, pp. 446-449. http://dx.doi.org/10.1109/LCN.2014.6925813.

[5] K. Suleiman, A. M. Taha and H. Hassanein. "Understanding the Interactions of Handover-Related Self-Organization Schemes," in *Proceedings of the 17th ACM international conference on Modeling, analysis and Simulation of Wireless and Mobile systems (MSWiM),* 2014, pp. 285-294. http://dx.doi.org/10.1145/2641798.2641830.

[6] 3GPP. "Evolved Universal Terrestrial Radio Access (E-UTRA) and Evolved Universal Terrestrial Radio Access Network (E-UTRAN); Overall description; Stage 2." TS 36.300, 3rd Generation Partnership Project (3GPP), Jun. 2011.

[7] 3GPP. "Technical Specification Group Radio Access Network; Evolved Universal Terrestrial Radio Access (E-UTRA); Radio Resource Control (RRC); Protocol specification (Release 10)." TS 36.331, 3rd Generation Partnership Project (3GPP), Jun. 2011.

[8] 3GPP. "Technical Specification Group Radio Access Network; User Equipment (UE) procedures in idle mode and procedures for cell reselection in connected mode (Release 10)." TS 25.304, 3rd Generation Partnership Project (3GPP), Jun. 2012.

[9] 3GPP. "Technical Specification Group Radio Access Network; Evolved Universal Terrestrial Radio Access (E-UTRA); User Equipment (UE) procedures in idle mode (Release 10)." TS 36.304, 3rd Generation Partnership Project (3GPP), Dec. 2011.

[10] 3GPP. "Technical Specification Group Services and System Aspects; Telecommunication Management; Self-Organizing Networks (SON); Concepts and requirements (Release 11)." TS 32.500, 3rd Generation Partnership Project (3GPP), Dec. 2011.

[11] T. Kürner, M. Amirijoo, I. Balan, H. Berg, A. Eisenblätter, T. Jansen, L. Jorguseski, R. Litjens, O. Linnell, A. Lobinger, M. Neuland, F. Phillipson, L. C. Schmelz, B. Sas, N. Scully, K. Spaey, S. Stefanski, J. Turk, U. Türke and K. Zetterberg. "Final Report on Self-Organisation and its Implications in Wireless Access Networks." Deliverable 5.9, *SOCRATES*, *EU Project,* Jan. 2010.

[12] L. C. Schmelz, M. Amirijoo, A. Eisenblätter, R. Litjens, M. Neuland and J. Turk. "A coordination framework for self-organisation in LTE networks," in *IFIP/IEEE International Symposium on Integrated Network Management (INM),* 2011, pp. 193-200. http://dx.doi.org/10.1109/INM.2011.5990691.

[13] A. Lobinger, S. Stefanski, T. Jansen and I. Balan. "Coordinating Handover Parameter Optimization and Load Balancing in LTE Self-Optimizing Networks," in *IEEE 73rd Vehicular Technology Conference (VTC),* 2011, pp. 1-5. http://dx.doi.org/10.1109/VETECS.2011.5956561.

[14] B. Sas, K. Spaey, I. Balan, K. Zetterberg and R. Litjens. "Self-Optimisation of Admission Control and Handover Parameters in LTE," in *IEEE 73rd Vehicular Technology Conference (VTC),* 2011, pp. 1-6. http://dx.doi.org/10.1109/VETECS.2011.5956153.

[15] H. Zhang, X. Wen, B. Wang, W. Zheng and Y. Sun. "A Novel Handover Mechanism Between Femtocell and Macrocell for LTE Based Networks," in *Second International Conference on Communication Software and Networks (ICCSN),* 2010, pp. 228-231. http://dx.doi.org/10.1109/ICCSN.2010.91.

[16] G. Yang, X. Wang and X. Chen. "Handover control for LTE femtocell networks," in *International Conference on Electronics, Communications and Control (ICECC),* 2011, pp. 2670-2673. http://dx.doi.org/10.1109/ICECC.2011.6067552.

[17] C. Feng, X. Ji and M. Peng. "Handover parameter optimization in self-organizing network," in *IET International Conference on Communication Technology and Application (ICCTA),* 2011, pp. 500-504. http://dx.doi.org/10.1049/cp.2011.0719.

[18] K. Kitagawa, T. Komine, T. Yamamoto and S. Konishi. "A handover optimization algorithm with mobility robustness for LTE systems," in *IEEE 22nd International Symposium on Personal Indoor and Mobile Radio Communications (PIMRC),* 2011, pp. 1647-1651. http://dx.doi.org/10.1109/PIMRC.2011.6139784.

[19] L. Ewe and H. Bakker. "Base station distributed handover optimization in LTE self-organizing networks," in *IEEE 22nd International Symposium on Personal Indoor and Mobile Radio Communications (PIMRC),* 2011, pp. 243-247. http://dx.doi.org/10.1109/PIMRC.2011.6139958.

[20] T. Jansen, I. Balan, J. Turk, I. Moerman and T. Kürner. "Handover Parameter Optimization in LTE Self-Organizing Networks," in *IEEE 72nd Vehicular Technology Conference (VTC),* 2010, pp. 1-5. http://dx.doi.org/10.1109/VETECF.2010.5594245.

[21] I. Balan, T. Jansen, B. Sas, I. Moerman and T. Kürner. "Enhanced weighted performance based handover optimization in LTE," in *Future Network and Mobile Summit,* 2011, pp. 1-8.

[22] I. M. Balan, I. Moerman, B. Sas and P. Demeester. "Signalling minimizing handover parameter optimization algorithm for LTE networks." *Wireless Networks Journal,* vol. 18, no. 3, pp. 295-306, Apr. 2012. http://dx.doi.org/10.1007/s11276-011-0400-5.

[23] S. S. Jeong, J. A. Han and W. S. Jeon. "Adaptive connection admission control scheme for high data rate mobile networks," in *IEEE 62nd Vehicular Technology Conference (VTC),* 2005, pp. 2607-2611. http://dx.doi.org/10.1109/VETECF.2005.1559021.

[24] Y. Zhang and D. Liu. "An adaptive algorithm for call admission control in wireless networks," in *IEEE Global Telecommunications Conference (GLOBECOM),* 2001, pp. 3628-3632. http://dx.doi.org/10.1109/GLOCOM.2001.966358.

[25] K. Spaey, B. Sas and C. Blondia. "Self-optimising call admission control for LTE downlink," presented at the Joint Workshop of COST 2100 SWG 3.1 & FP7-ICT-SOCRATES, Athens, Greece, 2010.

[26] F. Yu and V. C. M. Leung. "Mobility-based predictive call admission control and bandwidth reservation in wireless cellular networks," in *Proceedings of IEEE INFOCOM, 20th Annual Joint Conference of the Computer and Communications Societies,* 2001, pp. 518-526. http://dx.doi.org/10.1109/INFCOM.2001.916771.

[27] C. Oliveira, J. B. Kim and T. Suda. "An adaptive bandwidth reservation scheme for high-speed multimedia wireless networks." *IEEE Journal on Selected Areas in Communications*, vol. 16, no. 6, pp. 858-874, Aug. 1998. http://dx.doi.org/10.1109/49.709449.

[28] I. Ashraf, H. Claussen and L. T. W. Ho. "Distributed Radio Coverage Optimization in Enterprise Femtocell Networks," in *IEEE International Conference on Communications (ICC),* 2010, pp. 1-6. http://dx.doi.org/10.1109/ICC.2010.5502072.

[29] R. Kwan, R. Arnott, R. Paterson, R. Trivisonno and M. Kubota. "On Mobility Load Balancing for LTE Systems," in *IEEE 72nd Vehicular Technology Conference (VTC),* 2010, pp. 1-5. http://dx.doi.org/10.1109/VETECF.2010.5594565.

[30] P. Muñoz, R. Barco, I. De la Bandera, M. Toril and S. Luna-Ramirez. "Optimization of a Fuzzy Logic Controller for Handover-Based Load Balancing," in *IEEE 73rd Vehicular Technology Conference (VTC),* 2011, pp. 1-5. http://dx.doi.org/10.1109/VETECS.2011.5956148.

[31] H. Zhang, X. Qiu, L. Meng and X. Zhang. "Design of Distributed and Autonomic Load Balancing for Self-Organization LTE," in *IEEE 72nd Vehicular Technology Conference (VTC),* 2010, pp. 1-5. http://dx.doi.org/10.1109/VETECF.2010.5594567.

[32] J. M. R. Aviles, S. Luna-Ramirez, M. Toril, F. Ruiz, I. De la Bandera-Cascales and P. Munoz-Luengo. "Analysis of load sharing techniques in enterprise LTE femtocells," in *IEEE Wireless Advanced (WiAd),* 2011, pp. 195-200. http://dx.doi.org/10.1109/WiAd.2011.5983310.

[33] "Next Generation Mobile Networks: Radio Access Performance Evaluation Methodology." Next Generation Mobile Networks alliance (NGMN), Jan. 2008.

[34] K. Suleiman, "Interactions Study of Self Optimizing Schemes in LTE Femtocell Networks." M.A.Sc. thesis, Queen's University, Canada, 2012. http://hdl.handle.net/1974/7683.

[35] H. Claussen, L. T. W. Ho and L. G. Samuel. "Self-optimization of coverage for femtocell deployments," in *Wireless Telecommunications Symposium (WTS),* 2008, pp. 278-285. http://dx.doi.org/10.1109/WTS.2008.4547576.

[36] "Interference Management in OFDMA Femtocells." The Femto Forum, Mar. 2010.

[37] IEEE 802.16. "IEEE 802.16m Evaluation Methodology Document (EMD)." IEEE 802.16 Broadband Wireless Access Working Group, Jan. 2009.

[38] H. Kim, G. De Veciana, X. Yang and M. Venkatachalam. "Alpha-Optimal User Association and Cell Load Balancing in Wireless Networks," in *Proceedings of IEEE INFOCOM,* 2010, pp. 1-5. http://dx.doi.org/10.1109/INFCOM.2010.5462272.

[39] S. Sadr, A. Anpalagan and K. Raahemifar. "Radio Resource Allocation Algorithms for the Downlink of Multiuser OFDM Communication Systems." *IEEE Communications Surveys & Tutorials,* vol. 11, no. 3, pp. 92-106, 3rd Quarter 2009. http://dx.doi.org/10.1109/SURV.2009.090307.

[40] I. Viering, M. Dottling and A. Lobinger. "A Mathematical Perspective of Self-Optimizing Wireless Networks," in *IEEE International Conference on Communications (ICC),* 2009, pp. 1-6. http://dx.doi.org/10.1109/ICC.2009.5198628.

[41] M. Dirani and Z. Altman. "Self-organizing networks in next generation radio access networks: Application to fractional power control." *Computer Networks Journal,* vol. 55, no. 2, pp. 431-438, Feb. 2011. http://dx.doi.org/10.1016/j.comnet.2010.08.012.

[42] R. Nasri and Z. Altman. "Handover Adaptation for Dynamic Load Balancing in 3GPP Long Term Evolution Systems," in *International Conference on Advances in Mobile Computing and Multimedia (MoMM),* 2007, pp. 145-154.

[43] C. Mehlführer, M. Wrulich, J. C. Ikuno, D. Bosanska and M. Rupp. "Simulating the Long Term Evolution Physical Layer," in *Proceedings of the 17th European Signal Processing Conference (EUSIPCO),* 2009, pp. 1471-1478.

[44] "Simulation of Urban Mobility (SUMO)." Internet: http://sumo.sourceforge.net, Nov. 29, 2012 [Nov. 30, 2012].